Available online at https://rjas.rsu.ac.th
Formerly Rangsit Journal of Arts and Sciences (RJAS)

Journal of Current Science and Technology, January-June 2019 JCST Vol. 9 No. 1, pp. 29-39

ISSN 2630-0583 (Print)/ISSN 2630-0656 (Online)

Copper (II) adsorption property of 1D coordination polymer $[Cu_2(H_2O)(bipy)_2(tp)_2]$ (bipy = 2,2'-bipyridine, tp = terepthalate) after acid treatment

Winya Dungkaew[1*], Suwadee Jiajaroen[1, 2], Chatphorn Theppitak[2], Darunee Sertphon[3], and Kittipong Chainok[4]

[1]Department of Chemistry, Faculty of Science, Mahasarakham University, Kantarawichai, Maha Sarakham 44150, Thailand
[2]Department of Chemistry, Faculty of Science and Technology, Thammasat University, Pathum Thani 12121, Thailand
[3]Department of Chemistry, Faculty of Science, Rangsit University, Pathum Thani 12000, Thailand
[4]Materials and Textile Technology, Faculty of Science and Technology,Thammasat University, Pathum Thani 12121, Thailand

*Corresponding author; E-mail: winya.d@msu.ac.th

Received 13 April 2019, Revised 7 May 2019; Accepted 28 May 2019
Published online 18 June 2019

Abstract

A deep-blue crystal of terepthalato-bridged copper (II) coordination polymer (CP), $[Cu_2(H_2O)(bipy)_2(tp)_2]$ (**1**) was synthesized using hydrothermal reactions of $Cu(OAc)_2{\cdot}H_2O$, terephthalic acid (H_2tp), 2,2′-bipyridine (bipy), at pH ~8.45 in NH_4OH. Single crystal X-ray diffraction analysis at room temperature revealed that complex **1** crystallizes in monoclinic space group $P2_1/c$ with unit cell parameter a = 12.19720(10) Å, b = 14.78360(10) Å, c = 11.25080(10) Å, β = 91.5460(10)°, V = 2027.99(3) Å^3, and Z = 4. Complex **1** shows a one-dimensional zigzag chain along the [001] direction constructed by the tp^{2-} ligand linked to adjacent Cu^{2+} ions through the carboxylate groups, while the bipy acts as bidentate chelating ligand. Classical O–H···O hydrogen bonds are observed. The synthesized product was acid-treated via immersion in 1%v/v HNO_3, and within minute white crystals with retained morphology was obtained. Subsequently, the white acid-treated crystals were tested for their Cu^{2+} adsorption. Cu^{2+} adsorption of the white acid-treated crystals was fast and high. Adsorption as high as 214 mg Cu^{2+}/g adsorbent can be obtained from material prepared from acid treated of 1D polymeric chain.

Keywords: *after acid treatment, coordination polymer, Copper (II), Cu^{2+} adsorption, single crystal X-ray diffraction, terephthalic acid*

1. Introduction

A coordination polymer (CP) is a coordination compound that is constructed from metal ions and organic ligands through coordination of covalent bonds with repeating coordination entities extending in one- (1D), two- (2D) and three-dimensional (3D) structures (Batten et al., 2013). Among these, 2D or 3D CPs with potential void in the structure, the so called porous coordination polymers (PCPs) or metal-organic frameworks (MOFs), have been extensively studied due to their intriguing properties including designable porosity, internal pore surface functionality, and high surface area (Rowsell & Yaghi, 2004; Kitagawa, Kitaura, & Noro, 2004; Kitagawa & Matsuda, 2007; Noro, Kitagawa, Akutagawa, & Nakamura, 2009; Foo, Matsuda, & Kitagawa, 2014; Carn-Sanchez, Imaz, Stylianou, & Maspoch, 2014). These materials, to some extent, gain more interest over conventional natural-based or discovery-based synthetic compounds. Currently, PCP materials have become one of the most fast-growing research fields and many of these materials are being considered for potential applications in gas storage (Murray, Dinca, & Long, 2009; Hu & Zhang, 2010; Sculley, Yuan, & Zhou, 2011), chemical separations (Li, Kuppler, & Zhou, 2009; An, Geib, & Rosi, 2010; Bae, et al., 2010), chemical sensing (Allendorf, Bauer, Bhakta, & Houk, 2009), catalysis (Ma, Abney, & Lin, 2009; Lee, et al., 2009; Farha, Shultz, Sarjeant, Nguyen, & Hupp, 2011), ion exchange (An & Rosi, 2010), light harvesting (Lee, et al., 2011; Kent, et al., 2010), drug delivery (Horcajada, et al., 2006; Rocca, Liu, & Lin, 2011), and molecular adsorption (Han, et al., 2016; Luo, et al., 2016).

Apart from PCPs, nonporous CPs have rarely been explored for their adsorption properties. This may be due to their lack of porosity, which limits the applications mentioned above. Recently, acid etching has been reported as a method for hollowing out and fine tuning the porosity of the MOFs (Koo et al., 2017). This method is simply allowing generation of the pore size of the MOFs with increasing pore volume using acid diffusion into channels of MOFs. Consequently, mesopores are created that enhance mass transfer of large guest molecule into the pore surfaces of MOFs. This strategy provides an alternative route to synthesize suitable pore size MOF's beside conventional solvothermal methods. Taking into account this consideration, this work aims to study metal adsorption capability of nonporous CP after acid treatment. Thus, a simple 1D copper(II) based CP containing mixed ligands of terepthalate (tp) and 2,2'-bipyridine (bipy) was designed and synthesized. The H_2tp is easy to deprotonate under hydrothermal conditions and was selected as organic linker due to its various binding modes enabling connections with metal centers, as depicted in Figure 1 (Zhong, et al., 2012). The bipy molecule is known to be one of the most widely used ligands in crystallization applications due to its chelating ability, which could prevent the formation of 2D or 3D networks (Christian, Alexander, & Mir, 2000). Finally, Cu^{2+} adsorption capability of 1D CP after acid treatment was studied and the results discussed in detail.

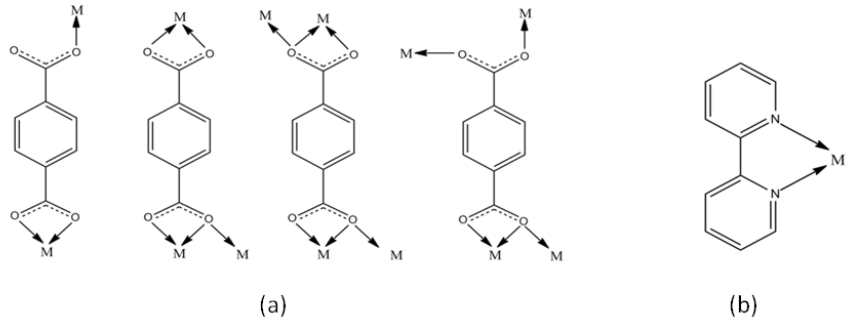

Figure 1 The binding modes of tp (a) and bipy (b) ligands

2. Materials and methods

2.1 Materials

Analytical grade $Cu(OAc)_2{\cdot}H_2O$ (JT Baker), bipyridine (Sigma-Aldrich), terephthalic acid (Sigma-Aldrich) were used without further purification. NH_4OH (Carlo Erba) was used for pH adjustment. HNO_3 (Carlo Erba) was used for acid treatment of the product and de-ionized water was used throughout the experiments.

2.2 Methods

2.2.1 Preparation of $[Cu_2(tp)_2(bipy)_2(H_2O)]$ (1)

Complex **1** was synthesized using a hydrothermal method. Typically, $Cu(OAc)_2{\cdot}H_2O$ (20 mg, 1 mmol), bipy (16 mg, 1 mmol), and H_2tp (17 mg, 1 mmol) in H_2O (10 mL) were mixed in 23 mL PTFE lined reactor. The mixture was adjusted to pH ~8.45 with NH_4OH, stirred for 15 min then covered with a PTFE cover, and tightened in stainless housing. The reactor was then heated in an oven at 160 °C for 24 h and then allowed to cool to room temperature. After filtration, deep blue block-shaped crystals of **1** were obtained, washed with water, and air-dried at room temperature.

The adsorbent was obtained from acid treatment of Complex **1**. Complex **1** was immersed in 1% v/v HNO_3 acid for a few minutes until the color changed from deep blue to white. The white product was then washed with water, filtered, and air-dried at room temperature before use in further experiments.

The morphology of the complex was observed by an Olympus SZX100 microscope and a JEOL scanning electron microscope. Phase identification was characterized using a Bruker D8 Quest XRD system. Thermal stability was studied by a TA instrument SDT Q600 TGA system. The FT-IR spectra were recorded on a Perkin-Elmer model Spectrum 100 spectrometer using ATR technique, in the range of 400–4000 cm^{-1}.

JCST Vol. 9 No. 1 Jan.-Jun. 2019, pp. 29-39
ISSN 2630-0583 (Print)/ISSN 2630-0656 (Online)

2.2.2 Adsorption study

The adsorbent was tested for its Cu^{2+} adsorption capability from copper aqueous solution. 10 mg of adsorbent was placed into 5.0 mL of 0.025 M, 0.050 M, 0.075 M, 0.10 M $Cu(OAc)_2 \cdot H_2O$ solution. The solutions were then allowed to stand at room temperature and Cu^{2+} adsorption monitored at 765 nm (λ_{max}) after 20, 40, 60, 80, 100, 120, and 140 min using a Thermo Scientific Genesys 20 spectrophotometer. The absorbance was recorded versus adsorption time.

2.2.3 X-ray crystal structure determination

Diffraction data were collected on a Bruker D8 QUEST CMOS diffractometer with graphite-monochromatic Mo-Kα radiation (λ = 0.71073 Å) operated at 296(2) K. Empirical absorption corrections were applied to data using SADABS (Bruker, 2014). The structure was solved by SHELXT-2015 (Sheldrick, 2015a) and refined by full-matrix least-squares based on F^2 using the SHELXL-97 (Sheldrick, 2015b) with Olex^2 (Dolomanov, Bourhis, Gildea, Howard, & Puschmann, 2009) as a graphics interface. Anisotropic displacement parameters were refined for all non-hydrogen atoms except for the disordered atoms. Hydrogen atoms were added theoretically. The crystallographic data for **1** is summarized in Table 1.

3. Result and discussion

The crystal morphology and habit of as-synthesized **1** is shown in Figure 2a. The crystal contains rod-like morphology, reasonably large in size with length about 500 μm. The colour change from deep blue crystal to white after acid treatment can be seen from Figure 2b. However, similar crystal morphology and size were retained.

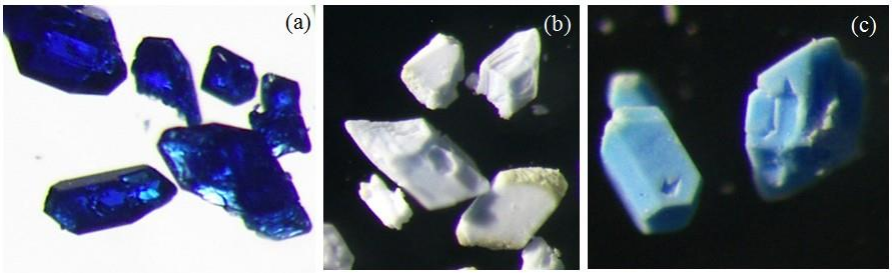

Figure 2 The morphology and appearance of (a) as-synthesized, (b) acid-treated adsorbent, and (c) adsorbent after Cu^{2+} resorption.

The single crystal X-ray diffraction analysis reveals that complex **1** crystallizes in the centrosymmetric monoclinic space group $P2_1/c$. The asymmetric unit contains two unique Cu^{2+} ions, one and two-half fully deprotonated tp^{2-} ligands, two bipy molecules and one lattice water molecule as shown in Figure 3. The central Cu1 atom is five-coordinated in a distorted square pyramidal geometry by three oxygen atoms from two tp^{2-} ligands and two nitrogen atoms for bipy molecule. The central Cu2 atom is also five-coordinated in a distorted square pyramidal geometry by two oxygen atoms from two tp^{2-} ligands, one oxygen atom from coordinated water molecule and two nitrogen atoms from bipy molecule. The Cu–O and Cu–N bond lengths are in the range 1.9384(8) – 2.4016(8) and 1.9871(10) – 2.0134(10) Å, respectively. Whereas, the O–Cu–O, N–Cu–N, and O–Cu–N bond angles are in the range 59.80(3) – 99.48(3)°, 80.45(4) – 81.59(4)°, and 91.17(4) – 173.51(4)°, respectively. As can be seen from Figure 4, two adjacent Cu^{2+} ions are linked together through the tp^{2-} ligands to form a one-dimensional zigzag chain along the [001] direction. Intrachain O–H···O hydrogen bonds between the coordinated water molecules and carboxylate groups are observed. The chains are further stacked into the 2D sheets via aromatic π-π interactions involving the bipy molecules with the centroid to centroid distances of 3.7907(6) Å.

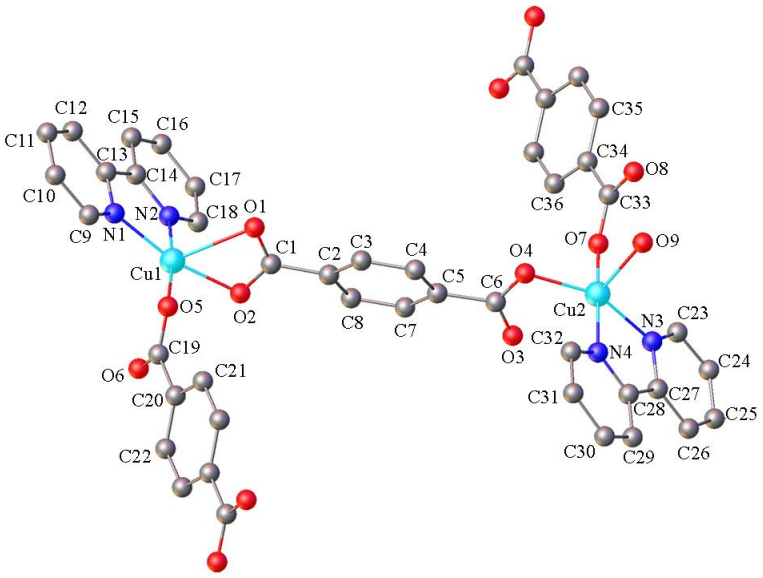

Figure 3 The molecular structure of **1**.

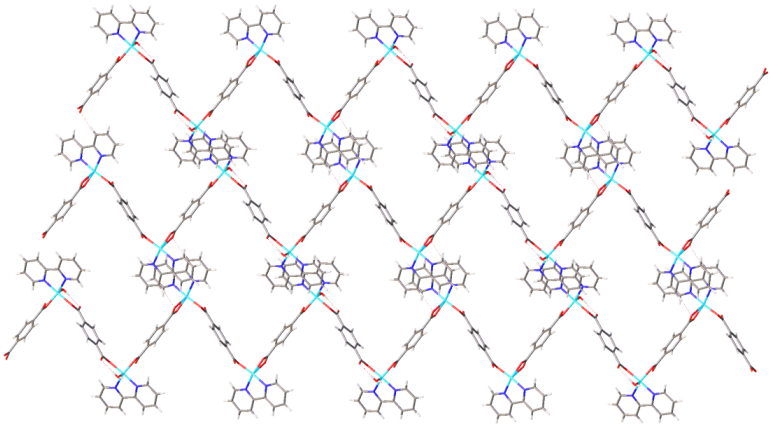

Figure 4 View of the 2D sheets of **1** along the [001] direction, constructed from the 1D chains are stacked through aromatic π-π interactions.

JCST Vol. 9 No. 1 Jan.-Jun. 2019, pp. 29-39
ISSN 2630-0583 (Print)/ISSN 2630-0656 (Online)

Table 1 Summary of crystallographic data of **1**.

Identification code	**1**
Formula	$C_{36}H_{26}Cu_2N_4O_9$
Formula weight	785
Temperature (K)	296(2)
Crystal system	Monoclinic
Space group	$P2_1/c$
a (Å)	13.66370(10)
b (Å)	17.18340(10)
c (Å)	14.08730(10)
β (°)	104.5889(8)
V (Å^3)	3200.90(4)
Z	4
ρ_{calc} (g·cm^{-3})	1.713
μ (mm^{-1})	2.196
F(000)	1679.0
Crystal size (mm^3)	0.22 × 0.18 × 0.12
Radiation	Mo K_α (λ = 0.71073 Å)
Reflections collected	18465
Independent reflections	6497
R_{int}, R_{sigma}	0.0139, 0.0150
Data/restraints/parameters	6497/2/616
Goodness-of-fit on F^2	1.033
R_1, wR_2 [$I > 2\sigma(I)$]	0.0209, 0.0508
R_1, wR_2 [all data]	0.0224, 0.0516
$\Delta\rho_{max}$, $\Delta\rho_{min}$ (e Å^{-3})	0.34, −0.22

The same amount of adsorbent (10 mg) was tested in four different Cu^{2+} concentrations (0.025 M, 0.05 M, 0.075 M and 0.10 M). The white crystals become light blue after resorption, representing the presence of copper in the material (Figure 2c). Comparable adsorption rates were observed from all systems, however a faster time to reach equilibrium was observed in the 0.025 M system (40 min) than other systems, while slowest time to equilibrium was observed in the 0.10 M system (80 min), Figure 5a. High adsorption capacity of 46, 87, 152, and 214 mg Cu^{2+}/g adsorbent were observed from 0.025 M, 0.050 M, 0.075 M, and 0.10 M systems, respectively, Figure 5b. It is suggesting that with the same amount of adsorbent, higher adsorption capability obtained from the system contains a higher concentration of adsorbate.

The comparison of Cu^{2+} adsorption capacity of various adsorbents from literature versus materials presented in this work is shown in Table 2. Materials presented in this work contains a relatively high adsorption capacity when compared to other class of materials such as zeolite, imprinted polymer, low-cost material, modified cyclodextrin, clay, and modified polymer. It should be noted here for comparison reasons that different adsorption conditions were studied i.e. temperature, pressure, and initial Cu^{2+} concentration may lead to different adsorption capacity obtained.

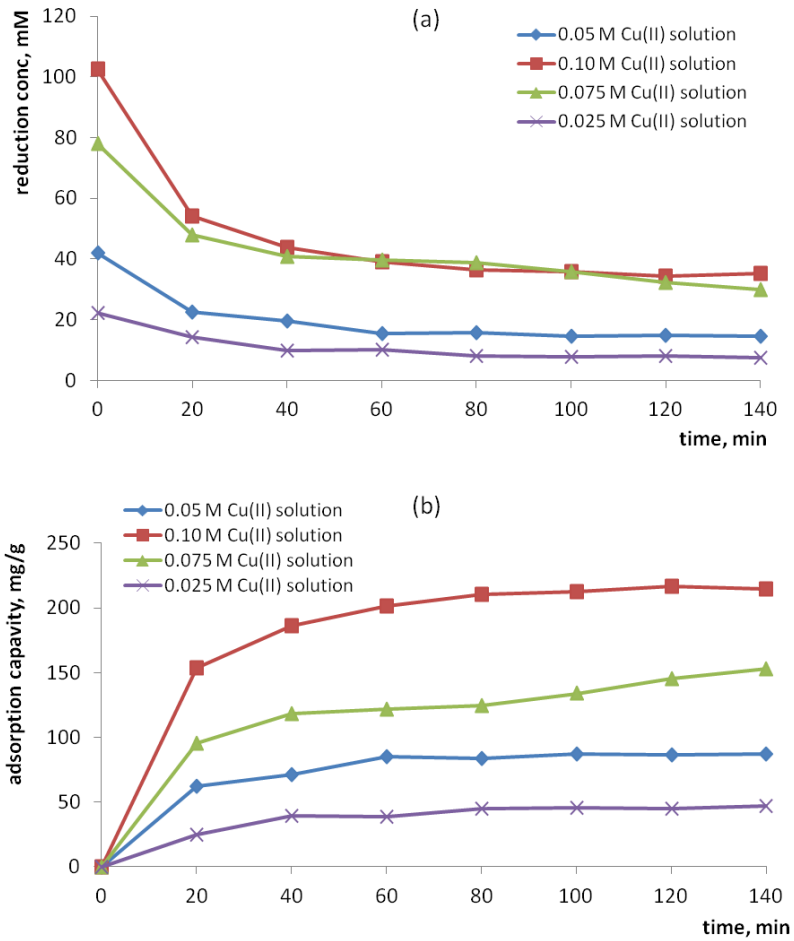

Figure 5 Adsorption capability of adsorbent obtained from acid-treated **1**.

Table 2 Compare sorption ability to other class of materials.

Materials	Range of adsorption capacity (mg Cu^{2+}/g)	References
Zeolite	0.37 – 47.50	(Babel & Kurniawan, 2003)
Imprinted polymer	16.55 – 132.77	(Erdem et al., 2018)
Shells of lentil, wheat, rice	2.95 – 17.42	(Aydin, Buluta, & Yerlikaya, 2007)
Low-cost materials	0.15 – 139	(Wan Ngah & Hanafiah, 2008)
CM-β-CD modified MNPs	47.20	(Badruddoza et al., 2011)
Clay	7 – 38	(Musso et al., 2014)
polyacrylate polymer	146	(Pietrelli et al., 2017)
Acid-treated **1**	47 – 214	This work

The SEM micrograph of the materials studied in this work is shown in Figure 6. The as-synthesized **1** contains a very smooth surface (Figure 6a). While, acid-treated adsorbent (Figure 6b) as well as adsorbent after Cu^{2+} resorption (Figure 6c) was found to be rough with small crevices on the surface which may due to acid etching effect. The surface area of the material is increased after acid treatment (Piscopo, Polyzoidis, Schwarzer, & Loebbecke, 2015) and thus may induce mass transfer of the ion between CP and solution enhancing fast adsorption capability.

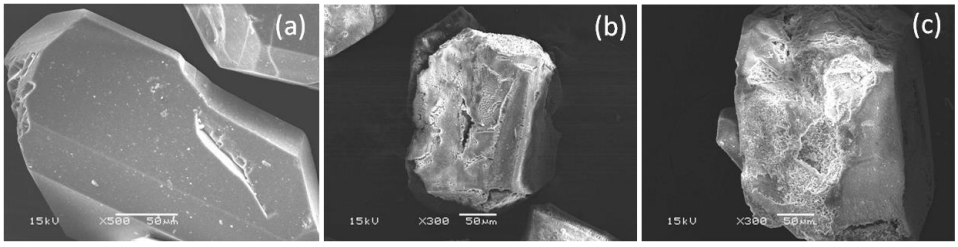

Figure 6 SEM micrograph of the surface of as-synthesized **1** (a), acid-treated adsorbent (b), and adsorbent after Cu^{2+} resorption (c).

Phase identification studies of as-synthesized **1**, acid-treated adsorbent, and adsorbent after Cu^{2+} resorption were carried out by PXRD analysis and the results are shown in Figure 7. The results suggest that a phase change occurred during these steps. Loss of several PXRD peaks was observed after acid treatment of **1**, perhaps because loss of the metal centre results in a less ordered structure. Therefore, far fewer PXRD peaks were found in acid-treated material compared to as-synthesized. However, the peak at 9 two-theta which corresponds to the presence of copper was found after resorption. To some extent, this indicates that copper was moved from the solution back to adsorbent at orderly position.

Thermogravimetric (TG) analysis of all samples was carried out under N_2 atmosphere and the TG curves are shown in Figure 8. The TG curve of as-synthesized **1** illustrates an initial weight loss of about 3% appearing from room temperature up to 140 ℃, corresponding to the release of coordinated water molecules. The framework is stable up to 280 °C, above which temperature the framework begins to collapse, accompanied by the decomposition of the organic components. The TG curve of the after-acid treatment sample is stable up to 230 ℃, and the decomposition takes place beyond this temperature. It is interesting to note that weight loss of acid treated adsorbent was observed to 100%, implying that no residue remain after decomposition after 330 °C. This may attribute to metal contents were completely removed after acid treatment remaining only organic part in the material (Koo, et al., 2017) which can be decomposed at such temperature. It is also evident that the deep blue crystal undergoes a change to white and the solution changes from clear to blue solution during the acid treatment experiment. In addition, the TG curves of the resorption samples are different to that of as-synthesized **1**, presumably because a new phase of copper complex is formed. This observation is in agreement with the PXRD analysis (Figure 7).

The chemical changes of the material were followed using FT-IR technique and the spectra are shown in Figure 9. The free C=O stretching of carboxylic acid is normally found at about 1,700 cm^{-1} (Tellez, et al., 2001), which corresponds to the peak found in adsorbent after acid was treated. No such peaks were found in both as-synthesized **1** and adsorbent after Cu^{2+} resorption, as this is represented that Cu^{2+} was originally bonded at C=O terminal of the carboxylate ligand. After acid was treated, Cu^{2+} was then removed and let to free the C=O, and then rebounded to C=O after Cu^{2+} resorption.

4. Conclusion

A new 1D copper(II) based CP with mixed terephthalate and bipy ligands of **1** was successfully synthesized under hydrothermal conditions. The solid-state structure of **1** is nonporous, however, the adsorption ability can be promoted by using acid treatment. This led to an empty metal site which was able to accept a high amount of Cu^{2+} resorption. This study demonstrated that as high as 214 mg Cu^{2+}/g adsorbent can be obtained from material prepared from acid treated of 1D chain CP.

5. Acknowledgement

The author would like to thank the Faculty of Science, Mahasarakham University for instrument support for PXRD characterization, Thammasat University for SCXRD analysis, and Rangsit University for FTIR characterization. We are also grateful for travel support from Mahasarakham University Development Fund and Dr. Adrian Roderick Plant, Division of Research Facilitation and dissemination, Mahasarakham University for his suggestions and English language support.

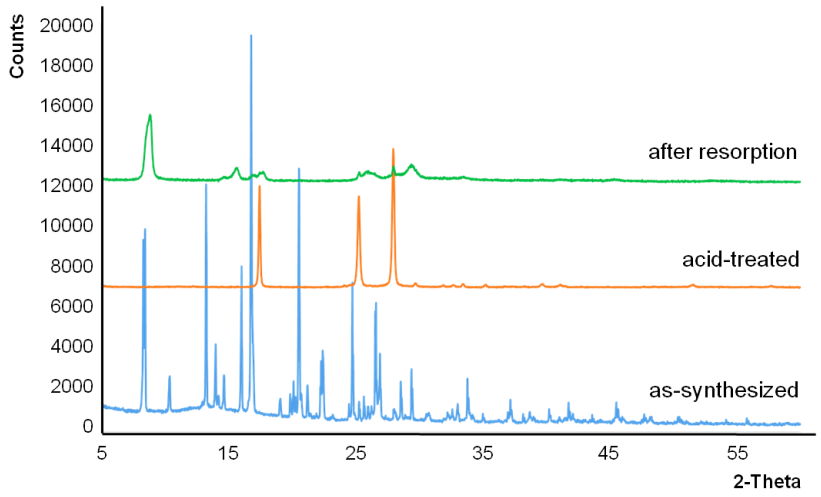

Figure 7 PXRD patterns of as-synthesized **1**, acid-treated adsorbent, and adsorbent after Cu^{2+} resorption.

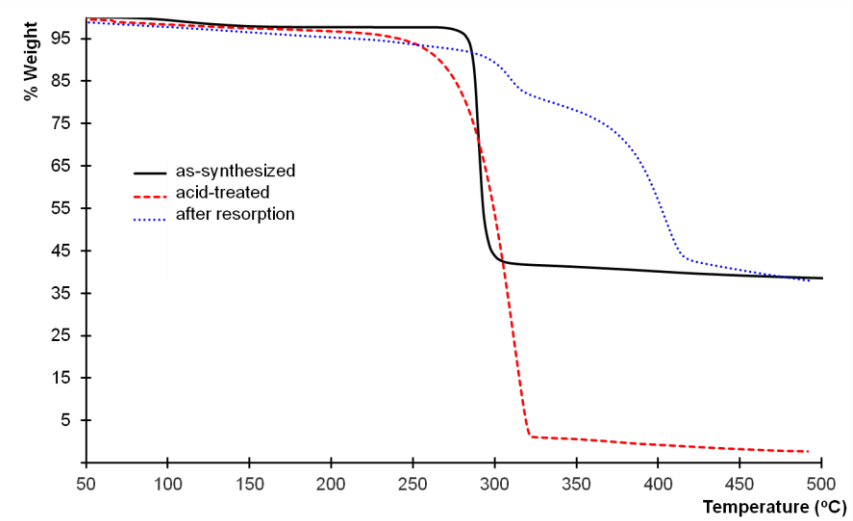

Figure 8 TGA curves of as-synthesized **1**, acid-treated adsorbent, and adsorbent after Cu^{2+} resorption.

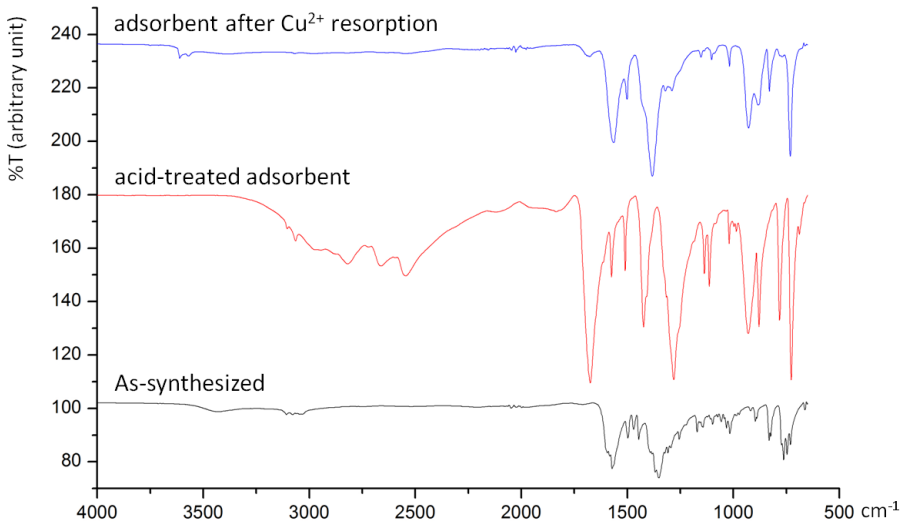

Figure 9 FTIR spectrum of as-synthesized **1**, acid-treated adsorbent, adsorbent after Cu^{2+} resorption.

6. References

Allendorf, M. D., Bauer, C. A., Bhakta, R. K., & Houk, R. J. T. (2009). Luminescent metal–organic frameworks. *Chemical Society Reviews*, *38*, 1330-1352. DOI: 10.1039/B802352M

An, J., Geib, S. J., Rosi, & N. L. (2010). High and Selective CO_2 Uptake in a Cobalt Adeninate Metal−Organic Framework Exhibiting Pyrimidine- and Amino-Decorated Pores. *Journal of the American Chemical Society*, *132*, 38-39. DOI: 10.1021/ja909169x

An, J., & Rosi, N. L. (2010). Tuning MOF CO_2 Adsorption Properties via Cation Exchange. *Journal of the American Chemical Society*, *132*, 5578-5779. DOI: 10.1021/ja1012992

Aydın, H., Buluta, Y., & Yerlikaya, C. (2007). Removal of copper (II) from aqueous solution by adsorption onto low-cost adsorbents. *Journal of Environmental Management*, *87*, 37-45. DOI: 10.1016/j.jenvman.2007.01.005

Babel, S., & Kurniawan, T. A. (2003). Low-cost adsorbents for heavy metals uptake from contaminated water: a review. *Journal of Hazardous Materials*, *97*, 219-243. DOI: 10.1016/S0304-3894(02)00263-7

Badruddoza, A. Z. M., Tay, A. S. H., Tan, P. Y., Hidajat, K., & Uddin, M. S. (2011). Carboxymethyl-β-cyclodextrin conjugated magnetic nanoparticles as nano-adsorbents for removal of copper ions: synthesis and adsorption studies. *Journal of Hazardous Materials*, *185*, 1177-1186. DOI: 10.1016/j.jhazmat.2010.10.029

Bae, Y.-S., Spokoyny, A. M., Farha, O. K., Snurr, R. Q., Hupp, J.T., & Mirkin, C. A. (2010). Separation of gas mixtures using Co(II) carborane-based porous coordination polymers. *Chemical Communications*, *46*, 3478-3480. DOI: 10.1039/B927499E

Batten, S, R., Champness, N. R., Chen, X. M., Garcia-Martinez, J., Kitagawa, S., Ohrstrom, L., . . . Reedijk, J. (2013). Terminology of metal-organic frameworks and coordination polymers. *Pure and Applied Chemistry*, *85*(8), 1715−1724. DOI: 10.1351/PAC-REC-12-11-20

Bruker (2014). APEX2, SADABS and SAINT. Madison, Wisconsin, USA: Bruker AXS Inc.

Carn-Sanchez, A., Imaz, I., Stylianou, K. C., & Maspoch, D. (2014). Metal–Organic Frameworks: From Molecules/Metal Ions to Crystals to Superstructures. *Chemistry - A European Journal*, *20*, 5192-5201. DOI: 10.1002/chem.201304529

Christian, K., Alexander, K., & Mir, W. H. (2000). Bipyridine: the most widely used ligand. A review of molecules comprising at least two 2,2'-bipyridine units. *Chemical Reviews*, *100*, 3353-3590. DOI: 10.1021/cr990376z

Dolomanov, O. V., Bourhis, L. J., Gildea, R. J., Howard, J. A. K., & Puschmann, H. (2009). OLEX2: a complete structure solution, refinement and analysis program. *Journal of Applied Crystallography*, *42*, 339-341. DOI: 10.1107/S0021889808042726

Erdem, O., Saylan, Y., Andaç, M., & Denizli, A. (2018). Molecularly Imprinted Polymers for Removal of Metal Ions: An Alternative Treatment Method. *Biomimetics*, *3*(4), 38. DOI: 10.3390/biomimetics3040038

Farha, O. K., Shultz, A. M., Sarjeant, A. A., Nguyen, S. T., & Hupp, J. T. (2011). Active-Site-Accessible, Porphyrinic Metal−Organic Framework Materials. *Journal of the American Chemical Society*, *133*, 5652-5655. DOI: 10.1021/ja111042f

Foo, M. L., Matsuda, R., & Kitagawa, S. (2014). Functional Hybrid Porous Coordination. *Chemistry of materials*, *26*, 310-322. DOI: 10.1021/cm402136z

Han, Y., Zheng, H., Liu, K., Wang, H., Huang, H., Xie, L. H., Wang, L., & Li, J. R. (2016). In-Situ Ligand Formation-Driven Preparation of a Heterometallic Metal–Organic Framework for Highly Selective Separation of Light Hydrocarbons and Efficient Mercury Adsorption. *ACS Applied Materials & Interfaces*, *8*, 23331-23337. DOI: 10.1021/acsami.6b08397

Horcajada, P., Serre, C., Vallet-Regí, M., Sebban, M., Taulelle, F., & Ferey, G. (2006). Metal-organic frameworks as efficient materials for drug delivery. *Angewandte Chemie, International Edition*, *45*, 5974-5978. DOI: 10.1002/anie.200601878

Hu, Y. H., & Zhang, L. (2010). Hydrogen storage in metal-organic frameworks. *Advanced Materials*, *22*, E117-130. DOI: 10.1021/cr200274s

Kent, C. A., Mehl, B. P., Ma, L., Papanikolas, J. M., Meyer, T. J., & Lin, W. (2010). Energy Transfer Dynamics in Metal−Organic Frameworks. *Journal of the American Chemical Society*, *132*, 12767-12769. DOI: 10.1021/ja102804s

Kitagawa, S., Kitaura, R., & Noro, S. (2004). Functional porous coordination polymers. *Angewandte Chemie (International ed. in English)*, *43*(18), 2334-2375. DOI: 10.1002/anie.200300610

Kitagawa, S., & Matsuda, R. (2007). Chemistry of coordination space of porous coordination polymers. *Coordination Chemistry Reviews*, *251*, 2490-2509. DOI: 10.1016/j.ccr.2007.07.009

Koo, J., Hwang, I. C., Yu, X., Saha, S., Kim, Y., & Kim, K. (2017). Hollowing out MOFs: hierarchical micro- and mesoporous MOFs with tailorable porosity via selective acid etching. *Chemical Science*, *8*, 6799-6803. DOI: 10.1039/C7SC02886E

Lee, J., Farha, O. K., Roberts, J., Scheidt, K. A., Nguyen, S. T., & Hupp, J. T. (2009). Metal–organic framework materials as catalysts. *Chemical Society Reviews*, *38*, 1450-1459. DOI: 10.1039/B807080F

Lee, C. Y., Farha, O. K., Hong, B. J., Sarjeant, A. A., Nguyen, S.T., & Hupp, J. T. (2011). Light-Harvesting Metal–Organic Frameworks (MOFs): Efficient Strut-to-Strut Energy Transfer in Bodipy and Porphyrin-Based MOFs. *Journal of the American Chemical Society*, *133*, 15858-15861. DOI: 10.1021/ja206029a

Li, J.-R., Kuppler, R. J., & Zhou, H.-C. (2009). Selective gas adsorption and separation in metal–organic frameworks. *Chemical Society Reviews*, *38*, 1477-1504. DOI: 10.1039/b802426j

Luo, X., Shen, T., Dng, L., Zhong, W., Luo, J., & Luo, S. (2016). Novel thymine-functionalized MIL-101 prepared by post-synthesis and enhanced removal of $Hg^{(2+)}$ from water. *Journal of Hazardous Materials*, *306*, 313-322. DOI: 10.1016/j.jhazmat.2015.12.034

Ma, L., Abney, C., & Lin, W. (2009). Enantioselective catalysis with homochiral metal–organic frameworks. *Chemical Society Reviews*, *38*, 1248-1256. DOI: 10.1039/B807083K

Murray, L. J., Dinca, M., & Long, J. R. (2009). Hydrogen storage in metal-organic frameworks. *Chemical Society Reviews*, *38*, 1294-1314. DOI: 10.1021/cr200274s

Musso, T. B., Parolo, M. E., Pettinari, G., & Francisca, F. M. (2014). Cu(II) and Zn(II) adsorption capacity of three different clay liner materials. *Journal of Environmental Management*, *146*, 50-58. DOI: 10.1016/j.jenvman.2014.07.026

Noro, S., Kitagawa, S., Akutagawa, T., & Nakamura, T. (2009). Coordination polymers constructed from transition metal ions and organic N-containing heterocyclic ligands: Crystal structures and microporous properties. *Progress in Polymer Science*, *34*(3), 240-279. DOI: 10.1016/j.progpolymsci.2008.09.002

Pietrelli, L., Palombo, M., Taresco, V., Crisante, F., Francolini, I., & Piozzi, A. (2017). Copper (II) adsorption capacity of a novel hydroxytyrosol-based polyacrylate. *Polymer Bulletin*, *74*(4), 1175-1191. DOI: 10.1007/s00289-016-1770-8

Piscopo, C. G., Polyzoidis, A., Schwarzer, & M., Loebbecke, S. (2015). Stability of UiO-66 under acidic treatment: Opportunities and limitations for post-synthetic modifications. *Microporous Mesoporous Mater*, 208, 30-35. DOI: 10.1016/j.micromeso.2015.01.032

Rocca, J. D., Liu, D., & Lin, W. (2011). Nanoscale Metal–Organic Frameworks for Biomedical Imaging and Drug Delivery. *Accounts of Chemical Research*, *44*, 957-968. DOI: 10.1021/ar200028a

Rowsell, J. L. C., & Yaghi, O. M. (2004). Metal–organic frameworks: a new class of porous materials. *Microporous and Mesoporous Materials, 73*, 3-14. DOI: 10.1016/j.micromeso.2004.03.034

Sculley, J., Yuan, D., & Zhou, H.-C. (2011). The current status of hydrogen storage in metal–organic frameworks—updated. *Environmental Engineering Science*, *4*, 2721-2735. DOI: 10.1039/C1EE01240A

Sheldrick, G. M. (2015a). SHELXT - Integrated space-group and crystal-structure determination. *Acta Crystallographica, Section A: Foundations of Crystallography*, *A71*, 3-8. DOI: 10.1107/S2053273314026370

Sheldrick, G. M. (2015b). Crystal structure refinement with SHELXL. *Acta Crystallographica, Section C: Crystal Structure Communications*, *C71*, 3-8. DOI: 10.1107/S2053229614024218

Tellez, C.A., Hollauer, E., Mondragon, M., & Castano, V.M. (2001). Fourier transform infrared and Raman spectra, vibrational assignment and ab initio calculations of terephthalic acid and related compounds. *Spectrochimica Acta, Part A: Molecular Spectroscopy*, *57*, 993-1007. DOI: 10.1016/S1386-1425(00)00428-5

Wan Ngah, W. S., & Hanafiah, M. A. (2008). Removal of heavy metal ions from wastewater by chemically modified plant wastes as adsorbents: a review. *Bioresource Technology*, *99*, 3935-3948. DOI: 10.1016/j.biortech.2007.06.011

Zhong, D. C., Ji-Hua, D., Xu-Zhong, L., Hui-Jin, L., Jin-Lian, Z., Ke-Jun, W., & Tong-Bu, L. (2012). Two Cadmium-Cluster-Based Metal–Organic Frameworks with Mixed Ligands of 1,2,3-Benzenetriazole (HBTA) and 1,4-Benzenedicarboxylic acid (H_2BDC). *Crystal Growth & Design*, *12*, 1992-1998. DOI: 10.1021/cg2016963